JOURNAL OF MATERIALS SCIENCE **36** (2001) 131–136

Evidence for microwave enhanced mass transport in the annealing of nanoporous alumina membranes

YU. V. BYKOV, S. V. EGOROV, A. G. EREMEEV, K. I. RYBAKOV, V. E. SEMENOV, A. A. SOROKIN
Institute of Applied Physics, Russian Academy of Sciences, Nizhny Novgorod, Russia
E-mail: rybakov@appl.sci-nnov.ru

S. A. GUSEV
Institute for Physics of Microstructures, Russian Academy of Sciences, Nizhny Novgorod, Russia

Results of a comparative study of pore evolution in nanostructured alumina membranes under annealing in a gyrotron microwave system and in conventional furnace are described. Microwave heating has resulted in an enhanced mass transport leading to reduction in the surface porosity of the membranes. Evolution patterns for the shape of individual pores are discussed and compared for microwave and conventional annealing. The notably different behavior of the pores suggests that microwave radiation provides an additional driving force for mass transport. The experimentally observed enhancement of mass transport appears to be stronger than predicted by the earlier proposed models.

1. Introduction

The problem of microwave enhanced mass transport in solids remains one of the most controversial issues in the microwave processing of materials. Many experimental studies have established the fact that the use of microwaves in high-temperature processes reduces the time and often the temperature needed for their completion [1]. The practical benefits are improved microstructure and properties of the materials produced with microwaves (e.g., microwave sintered ceramics [2]) and reduced energy consumption [3]. From the fundamental point of view, the mass transport enhancement phenomenon poses a challenging problem of identification of the mechanism responsible for it. While some hypotheses and theoretical models [4–8] have been already proposed, the phenomenon is still lacking accurate experimental characterization. Most of the evidence for the solid-state mass transport enhancement has been obtained in the experiments in microwave sintering of ceramics [9–11]. However, the complexity of ceramic microstructures and the presence of several diffusion mechanisms involved in sintering makes it difficult to identify experimentally the origin and nature of mass transport enhancement. This difficulty is aggravated by the fact that microwave heating, being of a volumetric nature, combined with peripheral heat losses results in temperature gradients across the ceramic samples. The temperature gradients themselves are known to be capable of enhancing the sintering process [12]. Therefore, identification of the nature of microwave mass transport enhancement requires careful de-convolution of thermal (resulting from temperature nonuniformity) and non-thermal (nonequilibrium, electromagnetic field-driven) effects. There have been studies in which temperature gradients similar to those of microwave heating were artificially created in the conventional heating experiments for comparison [11]. Another approach to distinguishing between thermal and nonthermal effects of microwaves is to reduce the impact of the temperature gradients that develop under microwave heating by choosing the appropriate experimental conditions and materials.

This paper describes a comparative study of pore structure evolution in nanostructured amorphous alumina membranes subjected to annealing in microwave field and in conventional oven. Investigation of the microwave effect on mass transport using porous membranes offers a number of important advantages over the microwave sintering experiments. The membranes, as described in detail below, comprise arrays of two-dimensional tubular pores, which are easy to characterize via surface porosity. The membrane annealing process is less complex than sintering with respect to the number of mass transport mechanisms involved simultaneously. The nanoscale pore sizes reduce temperature and/or time requirements for mass transport and allow statistical processing of the data on hundreds of pores in each electron microscopy image. Pure alumina is a well-characterized and chemically stable material, and its amorphous state in the membranes provides isotropy of the experimental system. Small dimensions of the membranes ensure uniformity of the electromagnetic

field acting on them. Finally, the small thickness of the membranes makes microwave heating effectively uniform in this particular case. Thus, the nanostructured alumina membranes are a suitable object for investigation of the nonthermal effect of microwave electromagnetic field on the mass transport in the solid state.

2. Experiment

The nanostructured amorphous alumina membranes obtained by an electrochemical process were provided by Dr. G. L. Hornyak of Colorado State University [13]. The porosity structure of the membranes before annealing is shown in Fig. 1. The average diameter of the pore channels was 60 nm, and membrane thickness was 25 μm. The pore channels initially had narrower "bottlenecks" near the membrane surface, with the average visible diameter of the pores equal to 55 nm. The average surface (visible) porosity was (21 ± 0.5)%. The typical dimensions of the membrane samples used in the experiments were about 2 mm $\times$ 2 mm.

Microwave annealing was done using a 10 kW (continuous operation) 30 GHz gyrotron system for microwave processing of materials [14]. The membrane samples were positioned in the focal area of the input microwave beam of linear polarization (Fig. 2) so that the orientation of the electric field vector was known. The beam had Gaussian intensity profile with the transverse diameter in the focal area about 40 mm. Annealing was done at constant heating rates in the range 7–90 °C/min with or without hold at the maximum temperature. The microwave power was controlled by a computerized power control loop using a type K thermocouple for sensing the membrane temperature. During annealing, the membranes were enclosed in a thermal insulation arrangement made of porous alumina and filled with loose alumina powder. The estimated field strength in the membranes was about

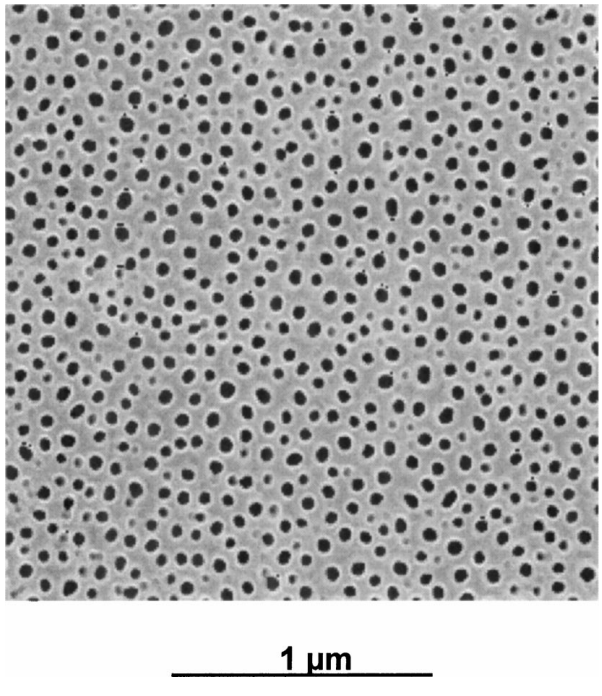

Figure 1 Porosity structure of alumina membranes before annealing.

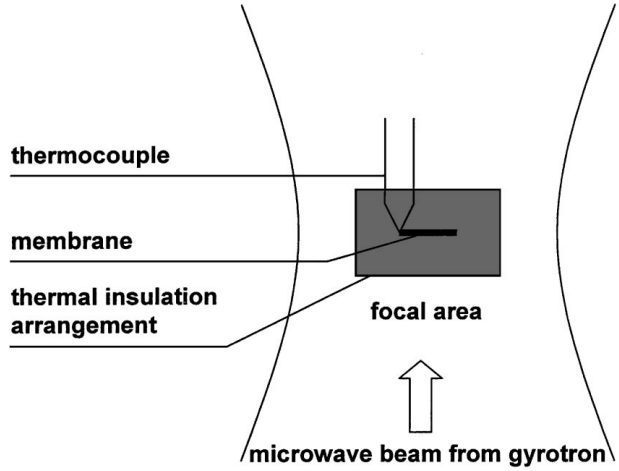

Figure 2 Experimental configuration schematic for microwave annealing.

3×10^4 V/m. Heating of the membranes resulted from both intrinsic microwave absorption in the membranes and in the thermal insulation arrangement components.

Conventional annealing was done in a resistive furnace. Heating schedules identical to those of microwave annealing were implemented by introducing the membranes controllably into the furnace preheated to the maximum temperature while monitoring the membrane temperature. For temperature sensing a thermocouple of the same type as in the microwave system was used.

The annealed membranes were characterized using scanning electron microscopy (SEM) and X-ray diffractometry (XRD). Surface porosity data were obtained by means of computer image analysis of SEM micrographs. In each image (similar to that shown in Fig. 1) there was approximately the same number of pores, 600 ± 25. The brightness distribution of all micrographs was bimodal, with the darker part of the distribution corresponding to pore interior and the brighter one corresponding to membrane surface. By measuring the proportion of the darker part of the brightness distribution the surface porosity was determined.

3. Results

For comparison between microwave and conventional annealing, the membranes were annealed at a heating rate of 30 °C/min up to maximum temperatures in the range of 900–1150 °C with a 1 hour hold at the maximum temperature. Fig. 3 shows the surface porosity of the annealed samples vs. hold temperature.

The results show that up to approximately 1000 °C there are no detectable changes in the porosity with neither microwave nor conventional annealing. In the temperature range between 1000 and 1150 °C conventional annealing still does not change the porosity significantly. However, microwave annealing results in a significant decrease in the porosity for this range of hold temperatures. Typical SEM images of the porosity structure of the membranes annealed conventionally and by microwaves are contrasted in Fig. 4. Image analysis shows that while the number of pores is approximately constant for all images, the size of pores

after microwave annealing significantly decreases. Image analysis has revealed no significant deviations in the average shape factor of all membranes, and no preferential direction of visible pore elongation was found.

Phase composition of the membranes was assessed by X-ray diffractometry. The analysis suggests that the initially amorphous material is partially transformed to the crystalline γ-Al_2O_3 phase at temperatures in the range 950–1150 °C. No quantitative information on the phase content was obtained due to low signal/noise ratio resulting from small dimensions of the membrane samples.

The next stage of experimental investigation was centered around microwave annealing with the maximum temperature of 1100 °C. Several annealing runs differing in the heating rate (7–90 °C/min) with or without hold at the maximum temperature were conducted. The porosity of the annealed membranes is plotted in Fig. 5 as a function of the time of exposure to temperatures above 1000 °C, in accordance with the previously mentioned fact that no pore evolution occurred below this temperature. Since, as noted above, the number of pores was approximately the same in all micrographs, a conclusion can be drawn that exposure to microwave irradiation results in consistent decrease in the average pore size.

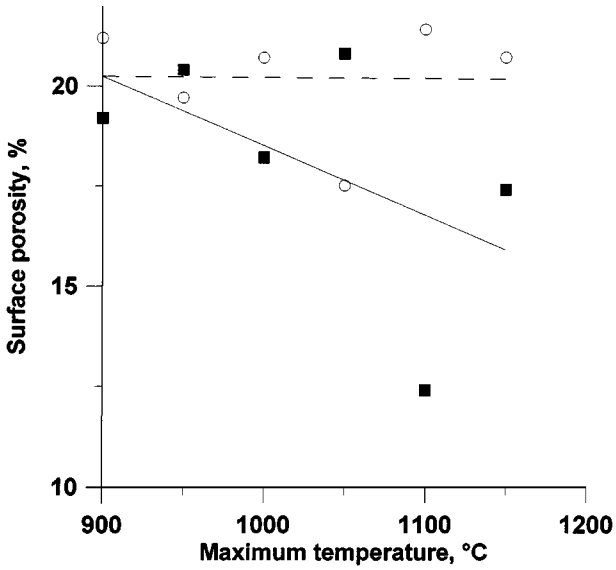

Figure 3 Surface porosity vs. maximum temperature of annealing: ■ – microwave annealing, ○ – conventional annealing. Heating rate was 30 °C/min and hold time was 1 hour in all cases.

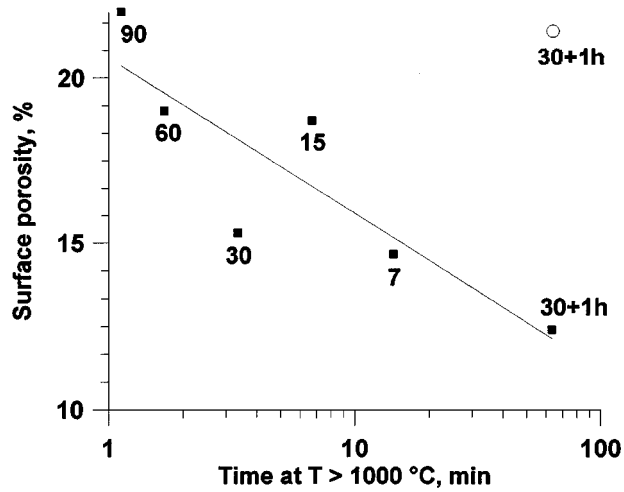

Figure 5 Surface porosity of alumina membranes vs. time of exposure to temperatures above 1000 °C: ■ – microwave annealing, ○ – conventional annealing. Heating rates (in °C/min) + hold times, if any, are shown for each annealing run. The maximum temperature of annealing was 1100 °C in all cases.

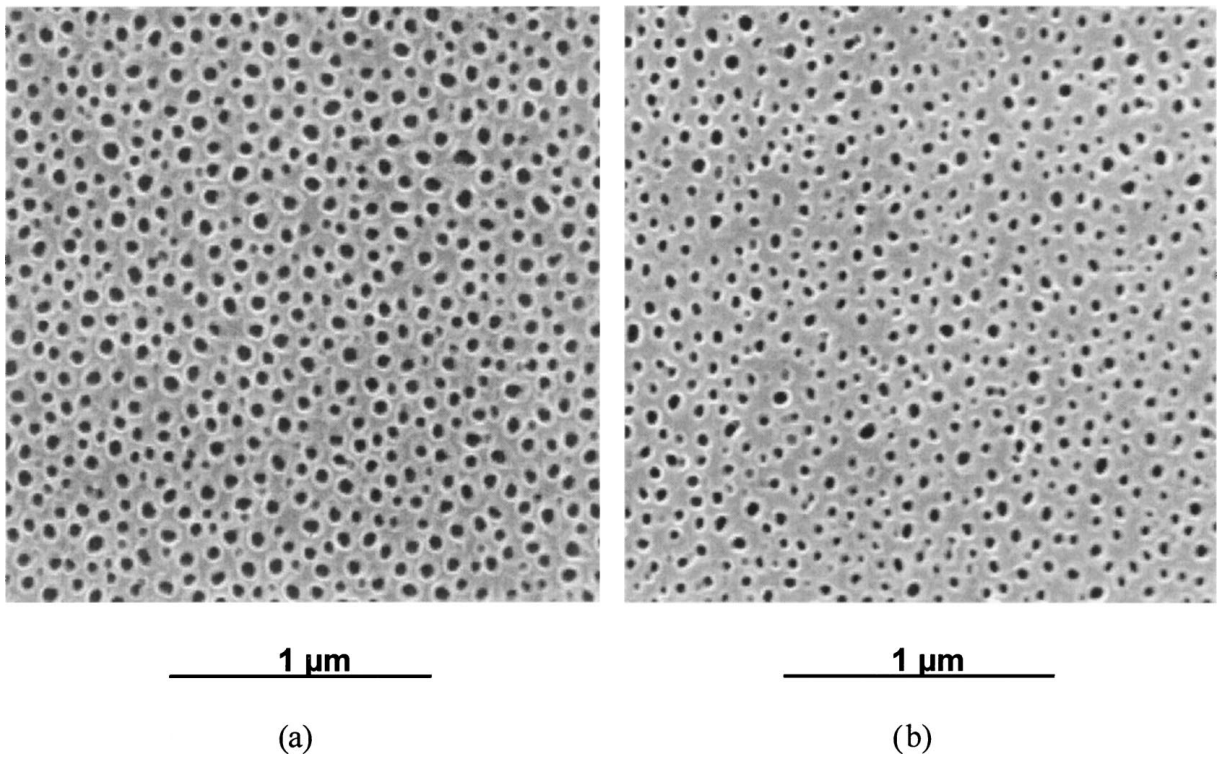

Figure 4 Porosity structure of alumina membranes: a) annealed conventionally at 1100 °C for 1 hour; b) annealed in microwave field at 1100°C for 1 hour.

4. Discussion

To obtain information about actual pore evolution during microwave annealing, the membrane micrographs were subjected to a detailed computer image analysis. Specifically, for each image, between the brightness levels corresponding to the pore interior (dark) and the membrane surface (bright) five intermediate brightness levels were chosen. These were assumed to reflect five depth levels on the bottleneck surface of the pores. The visible porosity was determined by analyzing brightness distributions using each of these five brightness levels as a threshold level. From these porosity data, the values of average pore radius at five depth levels were obtained for the microwave annealed membranes represented in Fig. 5.

The results of the analysis are shown in Figs 6 and 7. Fig. 6 shows the dependency of the average pore radius at five depth levels upon the time of exposure to temperatures above 1000 °C for the microwave annealing runs. It can be stated that the pore closure process propagates from the top region of the bottleneck surface downwards. Shown in Fig. 7 are the average profiles of the bottleneck surface of the pore for several instants of time. Since the average visible pore radius in the membranes before annealing was on the order of 30 nm, the average velocity of pore closure calculated from these results is on the order of 10^{-12}–10^{-11} m/s at different time intervals.

For identification of the mass transport path for the observed effect it should be noted that pore closure is observed under microwave heating at temperatures as low as 1000–1100 °C. Since no pore size reduction is observed below 1000 °C, it can be argued that the effect is based on a path with the lowest activation energy, viz. surface diffusion. Numerical simulation of pore evolution under the action of Laplace stresses via surface diffusion (which corresponds to the conventional annealing process) was undertaken in order to understand the difference made by microwave effects.

Simulation was done in cylindrical geometry. A tubular pore was considered surrounded by a column of solid material of a finite diameter. This configuration represented the pore array of the membrane, the column diameter playing the role of the half-distance between pore centers. Stages of the evolution of an initially cylindrical pore with flat top surface are shown in Fig. 8. A qualitative correlation of the simulated evolution pattern to the one obtained by the analysis of the experimental data can be done by comparing Figs 7 and 8. It can be seen that the pore assumes the bottleneck shape since the Laplace stresses tend to reduce the free surface, starting from the pore edge. This leads to a reduction in the minimum radius of pore, i.e., to

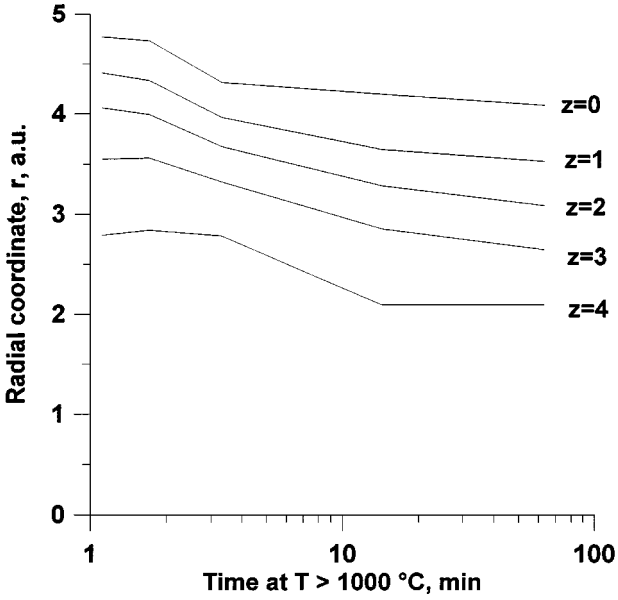

Figure 6 Radial coordinate obtained by image analysis, r, at five depth levels, z (z increases with depth), on the bottleneck surface of the pore vs. time of microwave exposure to temperatures above 1000 °C.

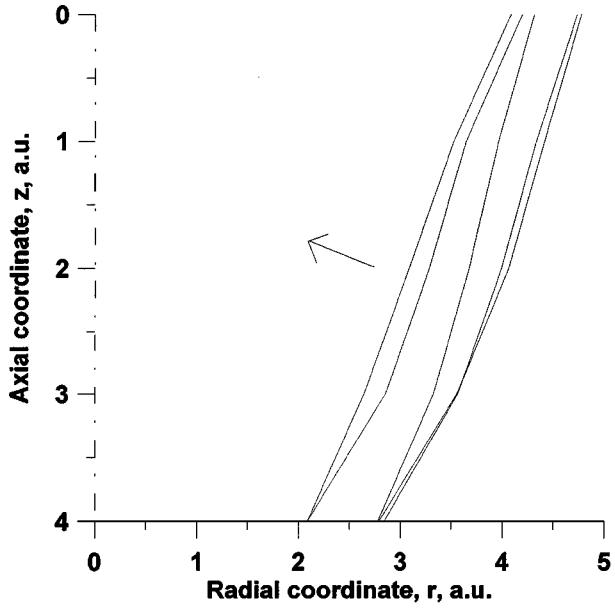

Figure 7 Average profiles of the bottleneck surface of the pore obtained by image analysis for several time instants corresponding to Fig. 5.

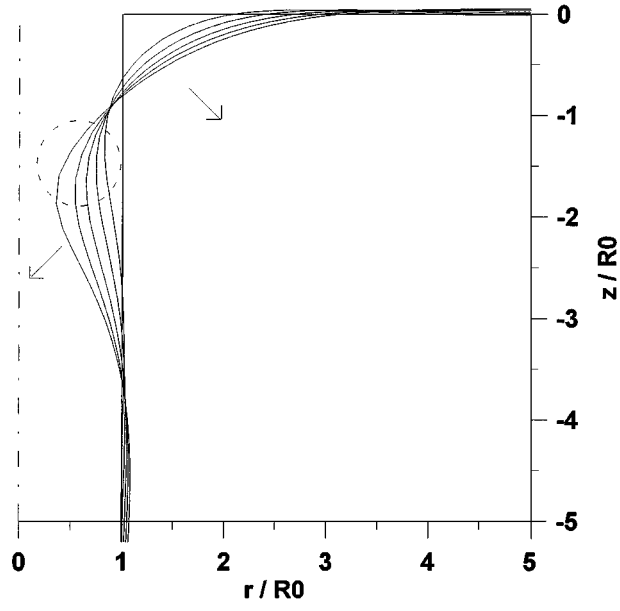

Figure 8 Simulated evolution of a tubular pore (of initial radius R_0) by surface diffusion. Pore surface profiles are shown for equidistant time instants. Interpore half-distance is $5R_0$. The bottleneck region that can be correlated to the pattern shown in Fig. 7 is encircled.

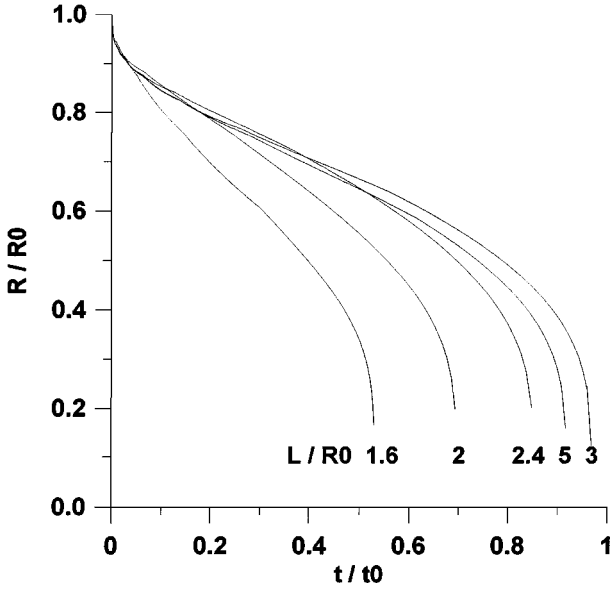

Figure 9 Calculated visible pore radius vs. normalized time for various half-distances, L, between pores.

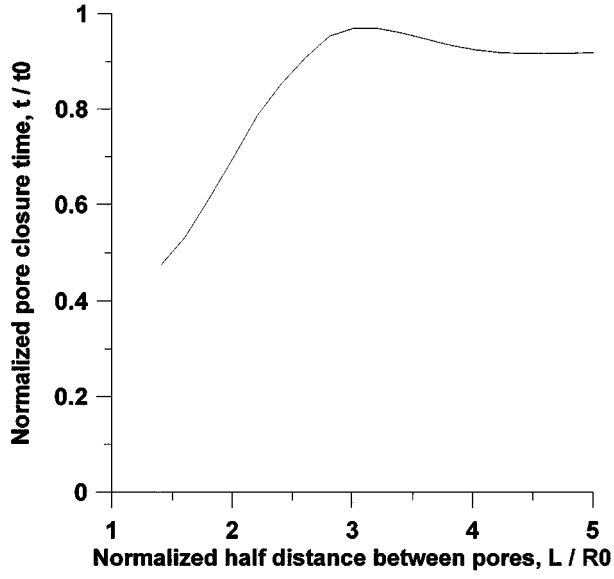

Figure 10 Pore closure time vs. half distance between pores.

the decrease in the visible pore size. The dependencies of pore radius on time are shown in Fig. 9. The characteristic time scale of the process is

$$t_0 = {R_0}^4 kT \big/ 2\gamma\Omega b N_0 D,$$

where R_0 is initial pore radius, k is Boltzmann's constant, T is absolute temperature, γ is coefficient of surface tension, Ω is vacancy volume, b is thickness of the layer in which surface diffusion occurs, N_0 is equilibrium vacancy concentration, and D is vacancy diffusivity. The velocity of pore closure, $\mathrm{d}R/\mathrm{d}t$, is very high at the initial stage when the curvature radius near the pore top is small. (This initial stage apparently occurs even during membrane storage at room temperature, which explains why the pores had the bottleneck shape initially, with $R/R_0 = 55$ nm/60 nm ≈ 0.92.) At the next stage, the pore surface has two oppositely directed curvature radii, which reduces the resulting Laplace stress and slows the mass transport down. Finally, when the pore radius is about 0.3 of the initial value, the "axial" curvature of pore becomes prevailing, and the pore comes to a complete closure. The time needed for the pore complete closure depends upon the interpore distance as shown in Fig. 10. The pore closure time exhibits a maximum when L, half interpore distance, is about 3 times pore radius, since the curvature at the top surface of the material compensates the "axial" curvature most effectively in that case.

Based on the simulation results, the velocity of pore closure can be estimated for conventional annealing. A reasonable estimate for the surface self-diffusion coefficient at 1100 °C in alumina is $N_0 D = 2 \times 10^{-19}$ m^2/s [15]. With $\gamma = 1$ J/m^2, $\Omega = 3 \times 10^{-29}$ m^3, kT = 2×10^{-20} J, $b = 10^{-9}$ m, $R_0 = 3 \times 10^{-8}$ m we obtain from the data shown in Fig. 7 that $\mathrm{d}R/\mathrm{d}t \cong 10^{-14}$ m/s. This correlates with the experimental fact that under conventional heating no detectable pore closure is observed during one hour holds at the maximum temperature. Yet, the fact that microwave annealing at the same temperature results in the pore closure velocities on the order of 10^{-12}–10^{-11} m/s suggests that exposure to microwave radiation enhances the mass transport significantly.

A widely discussed reason for microwave-enhanced mass transport is nonuniformity of temperature inherent in the microwave heating processes due to volumetric heat deposition and surface heat losses [16, 17]. An estimate for the resulting thermal stress is $K\alpha\Delta T$, where K is elastic compression modulus, α is coefficient of thermal expansion, and ΔT is temperature difference. The thermal stresses lead to additional transport of mass along the surface. The vacancy flux in the vicinity of a pore due to thermal stresses is

$$J = N_0 D K \alpha \Delta T \Omega / RkT,$$

and the resulting velocity of pore closure can be estimated as

$$\mathrm{d}R/\mathrm{d}t \cong bJ/R.$$

With $K = 10^{11}$ N/m^2 and $\alpha = 10^{-5}$ K^{-1} one can find that in order to provide the observed velocity of pore closure, the value of temperature gradient on the pore scale should be 10^{12} K/m. The enormity of this value suggests that temperature nonuniformity cannot be held responsible for the mass transport enhancement in the membranes. Thus, a conclusion about an additional driving force for mass transport arising from the action of microwave field can be drawn.

The observed enhancement of mass transport could be attributed to the rectified drift motion of charged vacancies in the microwave field. The possibility of partial rectification of the vacancy flux due to nonlinear ponderomotive field-vacancy interaction was shown in [5, 6]. The net drift flux of vacancies is

$$J = qD\langle NE\rangle / kT,$$

where q is effective electric charge of vacancies and $\langle NE\rangle$ is a time-averaged product of the vacancy concentration, N, perturbed by the electric field, E. The

resulting velocity of pore closure can be estimated as $dR/dt \cong bJ/R$. An analysis shows that the steady-state vacancy flows resulting from the ponderomotive effect can contribute to the pore closure process in the membranes. However, the efficiency of rectification, $\langle NE \rangle / (N_0 E_0)$, where E_0 is electric field amplitude inside the material (about 3×10^4 V/m), should be on the order of 1 to correlate with the value of pore closure velocity observed experimentally. That would mean that the alternating vacancy current induced by the microwave field along the surface is almost completely rectified, i.e., most of the vacancies present near the surface move during one phase of the field and stop during the other phase. The ponderomotive model as outlined in [5, 6] predicts a several orders of magnitude smaller rectification efficiency in the case of alumina, a material with low ionic conductivity. The field amplification effect due to microfocusing [8] is insignificant in the membrane configuration (as opposed to sintering) for all field polarizations. Thus, more work is needed to provide explanation and identify the mechanism for the microwave enhanced mass transport observed in the described experiments.

5. Conclusions

(1) A comparative study of pore evolution in nanostructured alumina membranes under annealing in a gyrotron microwave system and in conventional furnace has revealed significant difference between the processes accomplished with same temperature-time schedules.

(2) While no significant changes in the pore structure have been observed at conventional annealing with maximum temperatures up to 1150 °C and process times on the order of 1 hour, microwave annealing with maximum temperatures above 1000 °C has resulted in significant decrease in the average pore size. The effect has been found to be pronounced when the microwave electric field acting on the membranes is on the order of 3×10^4 V/m.

(3) The average pore size has been found to consistently decrease with increasing the duration of exposure to microwaves at temperatures above 1000 °C.

(4) The velocities of pore closure obtained from the experimental data exceed those obtained by means of surface diffusion simulation by 2–3 orders of magnitude.

(5) The observed enhancement of solid-state mass transport is not attributable to thermal stresses and apparently results from a non-thermal action of the microwave electric field.

Acknowledgement

This research is supported in part by the Commission of the European Communities under the Cooperation with Third Countries and International Organizations programme.

References

1. D. E. CLARK, W. H. SUTTON and D. A. LEWIS, in "Microwaves: Theory and Applications in Material Processing IV," edited by D. E. Clark, W. H. Sutton and D. A. Lewis (American Ceramic Society, Westerville, OH, 1997). Ceramic Transactions, Vol. 80, p. 61.
2. W. H. SUTTON, in "Microwave Processing of Materials III," edited by R. L. Beatty, W. H. Sutton and M. F. Iskander (Materials Research Society, Pittsburgh, 1992). Materials Research Society Symposium Proceedings, Vol. 269, p. 3.
3. M. C. L. PATTERSON, *et al., ibid.* p. 291.
4. J. H. BOOSKE, R. F. COOPER and I. DOBSON, *J. Mater. Res.* **7** (1992) 495.
5. K. I. RYBAKOV and V. E. SEMENOV, *Phys. Rev. B* **49** (1994) 64.
6. *Idem., ibid.* **52** (1995) 3030.
7. M. WILLERT-PORADA, in "Microwaves: Theory and Applications in Material Processing IV," edited by D. E. Clark, W. H. Sutton and D. A. Lewis (American Ceramic Society, Westerville, OH, 1997). Ceramic Transactions, Vol. 80, p. 153.
8. A. BIRNBOIM, J. P. CALAME and Y. CARMEL, *J. Appl. Phys.* **85** (1999) 478.
9. M. A. JANNEY and H. D. KIMREY, in "Microwave Processing of Materials, II," edited by W. B. Snyder, W. H. Sutton, M. F. Iskander and D. L. Johnson (Materials Research Society, Pittsburgh, 1990). Materials Research Society Symposium Proceedings, Vol. 189 p. 215.
10. R. WROE and A. T. ROWLEY, *J. Mater. Sci.* **31** (1996) 2019.
11. Y. BYKOV, A. EREMEEV and V. HOLOPTSEV, in "Microwave Processing of Materials, IV," edited by M. F. Iskander, R. J. Lauf and W. H. Sutton (Materials Research Society, Pittsburgh, 1994). Materials Research Society Symposium Proceedings, Vol. 347, p. 585.
12. D. BERUTO, R. BOTTER and A. W. SEARCY, *J. Amer. Ceram. Soc.* **72** (1989) 232.
13. G. L. HORNYAK, K. L. N. PHANI and D. L. KUNKEL, *et al., Nanostructured Materials* **6** (1995) 839.
14. Y. BYKOV, A. EREMEEV and V. FLYAGIN, *et al.*, in "Microwaves: Theory and Applications in Material Processing III," edited by D. E. Clark, D. C. Folz, S. J. Oda and R. Silberglitt (Amer. Ceram. Soc., Westerville, OH, 1995). Ceramic Transactions, Vol. 59, p. 133.
15. I. SAKAGUCHI, V. SRIKANTH, T. IKEGAMI and H. HANEDA, J. Amer. Ceram. Soc. **78** (1995) 2557.
16. D. L. JOHNSON, *ibid.* **74** (1991) 849.
17. K. I. RYBAKOV and V. E. SEMENOV, *Phil. Mag. A* **73** (1996) 295.

Received 20 September 1999
and accepted 15 June 2000